

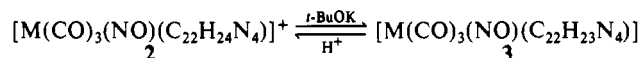
Contribution from URA CNRS 322, Université de Bretagne Occidentale, 29287 Brest-Cédex, France,  
and URA CNRS 254, Université de Rennes, 35042 Rennes-Cédex, France

## Molybdenum and Tungsten Complexes with Unusual Coordination Modes of a Dibenzotetraaza[14]annulene Ligand. From Bidentate to Tridentate Scorpiand Coordination by Reaction with Acetonitrile and from Bidentate to Tetradentate Coordination via Electrochemistry

Jean-Marc Giraudon,<sup>1a</sup> Dominique Mandon,<sup>1a,b</sup> Jean Sala-Pala,<sup>1a</sup> Jacques E. Guerschais,<sup>\*,1a</sup>  
Jean-Michel Kerbaol,<sup>1a</sup> Yves Le Mest,<sup>1a</sup> and Paul L'Haridon<sup>1c</sup>

Received November 21, 1988

Several aspects of the chemistry of the tetracarbonyl complexes  $[M(\text{CO})_4(\text{C}_{22}\text{H}_{24}\text{N}_4)]$  (**1a**,  $M = \text{W}$ ; **1b**,  $M = \text{Mo}$ ), in which the  $\text{N}_4$  macrocyclic molecule adopts an unusual bidentate coordination mode, have been developed.  $\text{NOBF}_4$  and  $\text{NOPF}_6$  react with **1** to produce the new cationic complexes  $[M(\text{CO})_3(\text{NO})(\text{C}_{22}\text{H}_{24}\text{N}_4)]\text{Y}$  (**2a**,  $M = \text{W}$ ,  $\text{Y} = \text{PF}_6$ ; **2b**,  $M = \text{Mo}$ ,  $\text{Y} = \text{BF}_4$ ; **2c**,  $M = \text{W}$ ,  $\text{Y} = \text{BF}_4$ ), which react with strong bases such as *t*-BuOK or BuLi to give the neutral complexes **3** via a reversible deprotonation with removal of one of the  $\text{CH}_2$  protons:

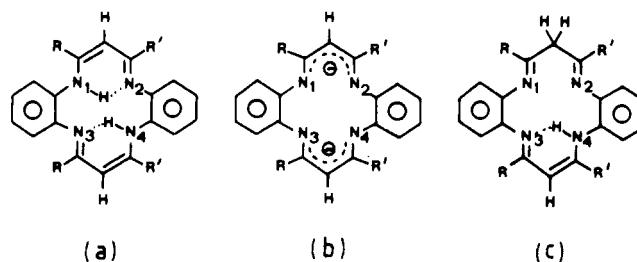


Reactions of complexes **2** with  $\text{CH}_3\text{CN}$  yield the new compounds  $[M(\text{CO})_3(\text{NO})(\text{C}_{24}\text{H}_{27}\text{N}_5)]\text{Y}$  (**4**) and correspond to the transformation of the bidentate ( $\text{N}_2$ ) ligand into a novel tridentate ( $\text{N}_3$ ) ligand. The structure of **4c** ( $M = \text{W}$ ,  $\text{Y} = \text{BF}_4$ ) has been determined by single-crystal X-ray diffraction analysis. The yellow crystals are triclinic, space group  $P\bar{1}$ , with  $a = 9.202$  (4) Å,  $b = 12.012$  (8) Å,  $c = 14.328$  (7) Å,  $\alpha = 95.74$  (5)°,  $\beta = 93.16$  (4)°,  $\gamma = 93.48$  (5)°,  $V = 1567$  Å<sup>3</sup>, and  $Z = 2$ . The structure was solved by using 2053 observed reflections and refined to  $R = 0.049$  and  $R_w = 0.064$ . In the complex cation the tungsten atom is seven-coordinate and has an irregular capped octahedral environment with the nitrosyl group in the capping position. Electrochemical studies of complexes **1** show that oxidation results in the formation of the cationic mononuclear oxo complexes  $[\text{MO}(\text{C}_{22}\text{H}_{22}\text{N}_4)]^+$  (**5a**,  $M = \text{W}$ ; **5b**,  $M = \text{Mo}$ ), in which the organic ligand adopts its usual tetradentate coordination mode. Electrolyses carried out in the presence of water indicate that  $\text{H}_2\text{O}$  is the oxygen source. A mechanism is presented for the transformation **1**  $\rightarrow$  **5**.

### Introduction

Dibenzotetraaza[14]annulene metal complexes constitute a well-studied class of coordination compounds.<sup>2-6</sup> Many of them exhibit interesting properties as electrocatalysts,<sup>7-9</sup> as models of biological systems,<sup>10</sup> and more recently as precursors for electrically conductive polymers.<sup>11-13</sup> In the large majority of these complexes, the  $\text{LH}_2$  dibenzotetraaza[14]annulene moiety acts as a simple tetradentate dianion ligand  $\text{L}^{2-}$ <sup>14-20</sup> (Chart I). In that sense, this

Chart I<sup>a</sup>



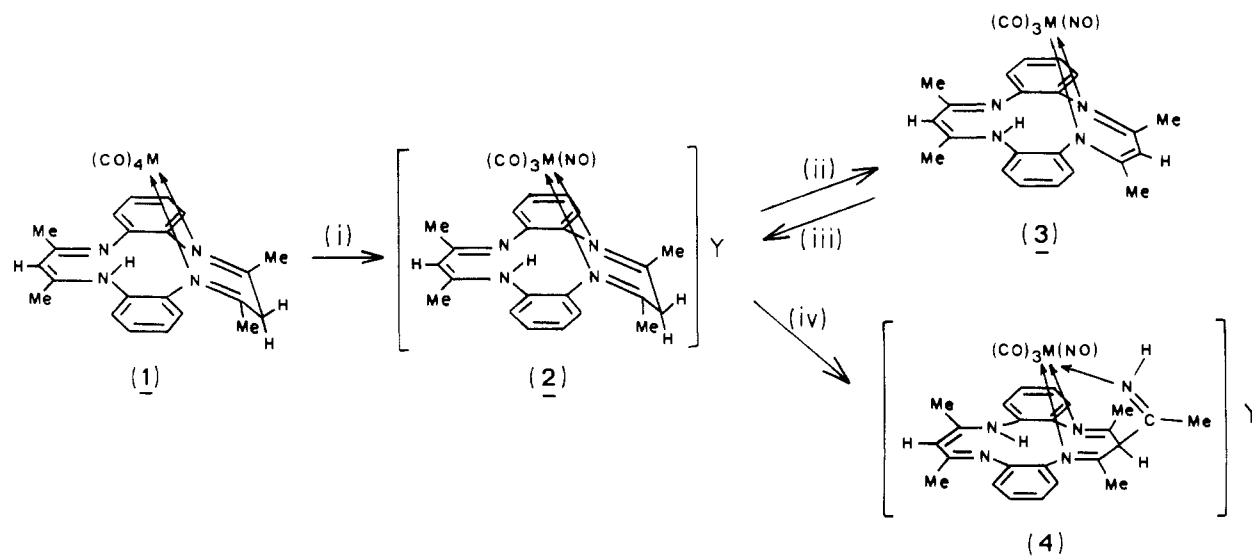
- (1) URA CNRS 322, Brest. (b) Present address: URA CNRS 424, Strasbourg. (c) URA CNRS 254, Rennes.
- Hiller, H.; Dimroth, P.; Pfitzner, H. *Liebigs Ann. Chem.* **1968**, 717, 137.
- Chave, P.; Honeybourne, C. L. *J. Chem. Soc., Chem. Commun.* **1969**, 279.
- Jäger, E. G. *Z. Anorg. Allg. Chem.* **1969**, 364, 177.
- Goedken, V. L.; Weiss, M. C. *Inorg. Synth.* **1980**, 20, 115.
- Cutler, A. R.; Alleyne, C. S.; Dolphin, D. *Inorg. Chem.* **1985**, 24, 2281.
- Beck, F. *Ber. Bunsen-Ges. Phys. Chem.* **1973**, 77, 353.
- Van den Brink, F.; Barendrecht, E.; Visscher, W. *Recl. Trav. Chim. Pays-Bas* **1980**, 99, 253.
- Bailey, C. L.; Bereman, R. D.; Rillema, D. P.; Nowak, R. *Inorg. Chem.* **1986**, 25, 933.
- Gottfried, V.; Weiss, A.; Dori, Z. *J. Am. Chem. Soc.* **1980**, 102, 3942.
- Hunziker, M.; Hilli, B.; Rihs, G. *Helv. Chim. Acta* **1981**, 64, 82.
- Majka, M.; Olech, Z.; Zyczkowska, T. *Pol. J. Chem.* **1984**, 53, 577.
- Hunziker, M.; Rihs, G. *Inorg. Chim. Acta* **1985**, 102, 39.
- Goedken, V. L.; Pluth, J. J.; Peng, S. M.; Bursten, B. *J. Am. Chem. Soc.* **1976**, 98, 8014.
- Weiss, M. C.; Bursten, B.; Peng, S. M.; Goedken, V. L. *J. Am. Chem. Soc.* **1976**, 98, 8021.
- Goedken, V. L.; Peng, S. M.; Molin-Morris, J. A.; Park, Y. *J. Am. Chem. Soc.* **1976**, 98, 8391.
- Weiss, M. C.; Gordon, G.; Goedken, V. L. *Inorg. Chem.* **1977**, 16, 305.
- Goedken, V. L.; Ladd, J. A. *J. Chem. Soc., Chem. Commun.* **1982**, 142.
- Yang, C. H.; Goedken, V. L. *J. Chem. Soc., Chem. Commun.* **1986**, 1101.
- Ciurli, S.; Floriani, C.; Chiesi-Villa, A.; Guastini, C. *J. Chem. Soc., Chem. Commun.* **1986**, 1401.

<sup>a</sup> Key: (a) initial organic  $\text{LH}_2$  molecule; (b) usual tetradentate  $\text{L}^{2-}$  ligand; (c) neutral and bidentate ( $\text{N}_1, \text{N}_2$ )  $\text{L}'\text{H}_2$  ligand found in **1**. In this work  $\text{R} = \text{R}' = \text{CH}_3$ .

ligand resembles a porphyrin; however, they both exhibit important differences with regard to electronic delocalization, core size, and framework flexibility.<sup>14</sup> This is clearly illustrated by their reactions with  $[\text{Mo}(\text{CO})_6]$ , which show striking differences: TPPH<sub>2</sub> (tetraphenylporphyrin) gives the quadruply bonded dinuclear complex  $[\text{Mo}(\text{TPP})]_2$ ,<sup>21</sup> while  $\text{LH}_2$  affords a tetracarbonyl complex  $[\text{Mo}(\text{CO})_4(\text{L}'\text{H}_2)]$ <sup>22,23</sup> (**1**) in which the  $\text{L}'\text{H}_2$  ligand arises from  $\text{LH}_2$  via a formal migration of a proton from the  $\text{N}_1$  to the CH unit (see Chart I). However, it must be pointed out that we have also been able to obtain the dinuclear complex  $[\text{MoL}]_2$  by reaction of  $[\text{Mo}_2(\text{OAc})_4]$  with  $\text{Li}_2\text{L}$ .<sup>24</sup>

Since the tetracarbonyl derivatives  $[\text{M}(\text{CO})_4(\text{L}'\text{H}_2)]$  (**1a**,  $M = \text{W}$ ; **1b**,  $M = \text{Mo}$ ) represent unique examples of complexes with

- (21) Yang, C. H.; Dzugan, S. J.; Goedken, V. L. *J. Chem. Soc., Chem. Commun.* **1986**, 1313.
- (22) Bell, L. G.; Dabrowiak, J. C. *J. Chem. Soc., Chem. Commun.* **1975**, 512.
- (23) Hashimoto, M.; Iwashita, H.; Gondo, K.; Sakata, K. *Kyushu Kogyo Daigaku Kenkyu Hokoku* **1985**, 51, 49.
- (24) Blake, A. J.; Holder, A. J.; Schröder, M.; Stephenson, T. A. *Acta Crystallogr.* **1984**, C40, 188.
- (25) Mandon, D.; Giraudon, J. M.; Toupet, L.; Sala-Pala, J.; Guerschais, J. E. *J. Am. Chem. Soc.* **1987**, 109, 3490.

Scheme 1<sup>a</sup>

<sup>a</sup> Conditions: (i) NOY in CH<sub>2</sub>Cl<sub>2</sub> (**2a**, M = W, Y = PF<sub>6</sub>; **2b**, M = Mo, Y = BF<sub>4</sub>; **2c**, M = W, Y = BF<sub>4</sub>); (ii) *t*-BuOK or BuLi in THF (**3a**, M = W; **3b**, M = Mo); (iii) HBF<sub>4</sub>·OEt<sub>2</sub> in THF or bubbling HCl gas (Y = Cl); (iv) CH<sub>3</sub>CN at room temperature (**4b**, M = Mo, Y = BF<sub>4</sub>; **4c**, M = W, Y = BF<sub>4</sub>).

the L'H<sub>2</sub> ligand, it appeared to us most important to explore further their reactivities. Particular attention has been given to the transformations of this N<sub>4</sub> molecule, acting as a neutral bidentate ligand, into (i) a N<sub>5</sub> molecule acting as a neutral tridentate unit by reaction with acetonitrile and (ii) the usual tetradentate L<sup>2-</sup> form via electrochemistry.

### Results

The transformations observed in this study are shown in Scheme I. The results of the structural and electrochemical studies are presented below.

**(1) Syntheses of the Cationic Nitrosyl Complexes 2.** Treatment at low temperature of a solution (CH<sub>2</sub>Cl<sub>2</sub>) of [W(CO)<sub>4</sub>(L'H<sub>2</sub>)] (**1a**) with NOPF<sub>6</sub> results in a purple solution from which purple microcrystalline product **2a** may be obtained in 80–90% yield. Formulation of **2a** as the cationic nitrosyl complex [W(CO)<sub>3</sub>(NO)(L'H<sub>2</sub>)](PF<sub>6</sub>) was deduced from analytical data and the IR spectrum (intense ν(NO) at 1650 cm<sup>-1</sup>; shift of the ν(CO) absorptions toward high frequency relative to the starting neutral complex **1a**). The high frequency corresponding to the ν(N=C≡C→C→N) vibration (1615 cm<sup>-1</sup>), associated with the presence in the <sup>1</sup>H NMR spectrum of an AB system, clearly suggests coordination of the organic ligand in its unusual bidentate L'H<sub>2</sub> mode, as in **1** (see Scheme I).

Similarly, reactions of the complexes **1** with NOBF<sub>4</sub> afford the corresponding tetrafluoroborate derivatives [M(CO)<sub>3</sub>(NO)(L'H<sub>2</sub>)](BF<sub>4</sub>) (**2b**, M = Mo; **2c**, M = W).

All these cationic complexes are thought to have a pseudooctahedral structure with the N<sub>4</sub> macrocycle acting as the L'H<sub>2</sub> bidentate ligand, but on consideration of the number, positions, and relative intensities of the IR carbonyl absorptions,<sup>25</sup> it appears impossible to choose between the *fac* and the *mer* structures.

**(2) Deprotonation of Complexes 2.** The reactions of complexes **2** with strong organic bases such as *t*-BuOK or BuLi are not clean and lead to the formation of the slightly impure products **3** in low yield. Proton NMR data, which show the presence of an N–H signal at δ 13.0 ppm and disappearance of the AB spectrum assignable to a CH<sub>2</sub> group in **2**, and IR data (absence of ν̄(BF<sub>4</sub>) or ν̄(PF<sub>6</sub>)) are indicative of a nonionic structure resulting from a proton abstraction from the methylene site according to eq ii of Scheme I. This structural hypothesis is supported by the fact that reaction of **3** with HBF<sub>4</sub>·OEt<sub>2</sub> or HCl gas in THF solution at low temperature regenerates the initial cation, showing the

deprotonation of **2** is reversible.

**(3) Reaction of Complexes 2 with CH<sub>3</sub>CN.** Although the complexes **2** are readily soluble in acetonitrile, the initial clear solutions, after standing a few hours, deposit microcrystals of the novel complexes **4**. The yellow complex **4c**, obtained from the purple derivative [W(CO)<sub>3</sub>(NO)(L'H<sub>2</sub>)](BF<sub>4</sub>) (**2c**), gives analytical results corresponding to the formation of a 2:1 complex between CH<sub>3</sub>CN and **2c**. Although the IR spectrum of **4c** shows strong similarities with that of **2c** [IR (cm<sup>-1</sup>): **4c**, 2010 s and 1935 vs ν(CO), 1670 s ν(NO), 1070 vs br ν(BF); **2c**, 2015 s and 1920 vs ν(CO), 1640 s ν(NO), 1070 vs br ν(BF)], the <sup>1</sup>H NMR spectra exhibit striking differences: (i) two N–H signals, and not one as observed in **2c**, are observed downfield at δ 11.96 and 12.80 ppm for **4c**; (ii) the AB system corresponding to the CH<sub>2</sub> moiety in **2** does not appear for **4**. As these spectroscopic data suggest the "insertion" of a CH<sub>3</sub>CN molecule into a C–H bond of the CH<sub>2</sub> group of **2** [see reaction iv, Scheme I], an X-ray study was undertaken; the results (see section 4) confirm the formulated hypothesis.

Formation of the seven-coordinate cationic complexes **4** is remarkable because of the mild conditions employed (acetonitrile at room temperature) to transform the starting bidentate ligand into a novel tridentate ligand. Rather than an easy insertion of the C≡N bond of an acetonitrile molecule into a covalent CH bond, reaction iv could indicate the easy ionization of a proton from the CH<sub>2</sub> moiety of the cationic complexes **2**. It is noteworthy that reaction with acetonitrile only occurred with the tricarbonyl nitrosyl cations **2** and was not observed with the starting neutral tetracarbonyl derivatives **1**, which could be recrystallized from this solvent. Reaction iv may be compared to an earlier study, in which a hexacoordinate iron compound containing a novel hexadentate N<sub>6</sub> ligand was obtained by reaction in acetonitrile of [Fe(CH<sub>3</sub>CN)<sub>6</sub>]<sup>2+</sup> with a usually tetradentate N<sub>4</sub> ligand.<sup>26</sup> With the tetramethyldibenzotetraaza[14]annulene ligand L<sup>2-</sup>, the cobalt(II) complex [Co(C<sub>22</sub>H<sub>22</sub>N<sub>4</sub>)] readily adds, under acidic conditions, one molecule of a wide variety of nitriles (RC≡N) to give the cationic complexes [Co(RC<sub>23</sub>H<sub>23</sub>N<sub>5</sub>)]<sup>+</sup> containing a new pentadentate macrocyclic ligand.<sup>27</sup> While subsequent addition of a base to this new cobalt complex regenerated the starting compound [CoL],<sup>27</sup> **4c** reacts with *t*-BuO<sup>-</sup> in THF to give complex [W(CO)<sub>3</sub>(NO)(L'H)] (**3a**). Associated with other recent work,<sup>28</sup>

(25) Condon, D.; Deane, M. E.; Lalor, F. J.; Connelly, N. G.; Lewis, A. C. *J. Chem. Soc., Dalton Trans.* **1977**, 925.

(26) Bowman, K.; Riley, D. P.; Bush, D. H. *J. Am. Chem. Soc.* **1975**, 97, 5036.

(27) Weiss, M. C.; Goedken, V. L. *J. Am. Chem. Soc.* **1976**, 98, 3389.

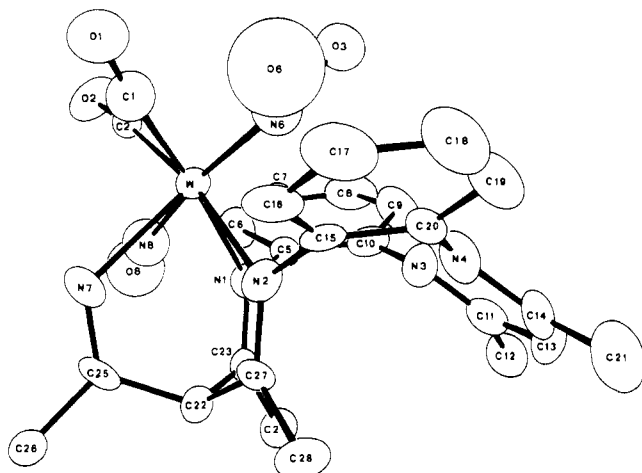


Figure 1. ORTEP plot of the complex cation found in **4c** (50% probability ellipsoids), showing the two positions of the nitrosyl group (statistical occupancy factors of 0.5).

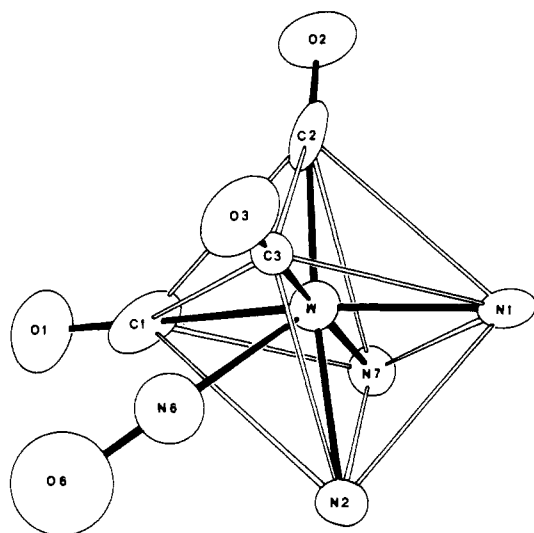


Figure 2. Coordination sphere of the tungsten atom with the nitrosyl group in the N(6)-O(6) position.

Table I. Crystal and Refinement Data for  $[\text{W}(\text{CO})_3(\text{NO})(\text{C}_{24}\text{H}_{27}\text{N}_5)](\text{BF}_4)\cdot\text{CH}_3\text{CN}$  (**4c**)

empirical formula	$\text{C}_{27}\text{H}_{27}\text{N}_6\text{O}_4\text{W}\cdot\text{BF}_4\cdot\text{CH}_3\text{CN}$
fw	811.25
cryst syst	triclinic
lattice params	$a = 9.202(4) \text{ \AA}$ $b = 12.012(8) \text{ \AA}$ $c = 14.328(7) \text{ \AA}$ $\alpha = 95.74(5)^\circ$ $\beta = 93.16(4)^\circ$ $\gamma = 93.48(5)^\circ$ $V = 1567 \text{ \AA}^3$
space group	$P\bar{1}$
Z	2
$d(\text{calc})$	$1.719 \text{ g/cm}^3$
$F(000)$	800
radiation	Mo $K\alpha$ ( $\lambda = 0.71069 \text{ \AA}$ ) graphite monochromated
$\mu(\text{Mo } K\alpha)$	$38.31 \text{ cm}^{-1}$
diffractometer	Enraf-Nonius CAD4
$2\theta_{\text{max}}$	$64^\circ$
no. of observns with $I > 3\sigma(I)$	2053
no. of variables	409
R	0.049
$R_w^a$	0.064
goodness of fit indicator	1.8

$$^a w = 1/\sigma(F_o)^2 = [\sigma^2(I) + (0.07F_o)^2]^{-1/2}$$

the reaction reported here extends the already rich reactivity of acetonitrile toward coordination compounds.

Table II. Final Fractional Atomic Coordinates and  $B$  ( $\text{\AA}^2$ ) Values for Non-Hydrogen atoms of  $[\text{W}(\text{CO})_3(\text{NO})(\text{C}_{24}\text{H}_{27}\text{N}_5)](\text{BF}_4)\cdot\text{CH}_3\text{CN}$  (**4c**)

atom	x	y	z	$B^a$
W	0.10114 (6)	0.22457 (5)	0.25719 (4)	2.47 (1)
F(1)	0.181 (2)	0.116 (1)	-0.0449 (7)	8.5 (3)
F(2)	0.166 (1)	0.072 (2)	-0.2010 (8)	10.7 (4)
F(3)	0.332 (2)	0.192 (1)	-0.1409 (9)	15.2 (4)
F(4)	0.344 (2)	0.028 (2)	-0.109 (1)	16.6 (5)
O(1)	-0.129 (1)	0.138 (1)	0.3913 (8)	5.3 (3)
O(2)	-0.152 (1)	0.286 (1)	0.1176 (8)	4.7 (3)
O(3)	0.102 (1)	0.450 (1)	0.3687 (9)	5.7 (3)
N(1)	0.273 (1)	0.2679 (9)	0.1655 (7)	2.2 (2)
N(2)	0.292 (1)	0.158 (1)	0.3305 (8)	3.0 (3)
N(3)	0.457 (2)	0.436 (1)	0.2611 (8)	4.0 (3)
N(4)	0.471 (1)	0.340 (1)	0.4175 (8)	3.9 (3)
N(5)	0.228 (2)	0.861 (1)	0.313 (1)	7.5 (5)
N(7)	0.103 (1)	0.0625 (9)	0.1749 (7)	2.8 (3)
C(1)	-0.044 (2)	0.167 (1)	0.339 (1)	3.9 (4)
C(2)	-0.066 (2)	0.264 (1)	0.1732 (9)	2.9 (3)
C(3)	0.104 (1)	0.362 (1)	0.3242 (8)	1.9 (2)*
C(5)	0.279 (2)	0.381 (1)	0.131 (1)	3.5 (3)
C(6)	0.188 (2)	0.398 (1)	0.055 (1)	3.3 (3)
C(7)	0.192 (2)	0.507 (1)	0.030 (1)	4.1 (4)
C(8)	0.280 (2)	0.594 (1)	0.076 (1)	4.2 (4)
C(9)	0.369 (2)	0.573 (1)	0.155 (1)	4.9 (4)
C(10)	0.374 (2)	0.466 (1)	0.183 (1)	3.7 (4)
C(11)	0.597 (2)	0.461 (1)	0.274 (1)	4.1 (4)
C(12)	0.686 (2)	0.518 (1)	0.204 (1)	5.1 (4)
C(13)	0.674 (2)	0.430 (1)	0.357 (1)	3.9 (4)
C(14)	0.614 (2)	0.374 (1)	0.427 (1)	4.9 (4)
C(15)	0.304 (1)	0.179 (1)	0.4342 (9)	2.4 (3)
C(16)	0.228 (2)	0.109 (1)	0.485 (1)	4.0 (4)
C(17)	0.240 (2)	0.128 (1)	0.582 (1)	4.4 (4)
C(18)	0.331 (2)	0.214 (2)	0.623 (1)	5.1 (4)
C(19)	0.406 (2)	0.285 (1)	0.574 (1)	4.5 (4)
C(20)	0.396 (2)	0.268 (1)	0.4749 (9)	3.5 (3)
C(21)	0.713 (2)	0.339 (2)	0.508 (1)	5.5 (5)
C(22)	0.364 (2)	0.087 (1)	0.1764 (9)	3.1 (3)
C(23)	0.371 (1)	0.201 (1)	0.1418 (9)	2.2 (3)
C(24)	0.498 (2)	0.227 (1)	0.084 (1)	4.5 (4)
C(25)	0.221 (2)	0.022 (1)	0.1485 (9)	3.1 (3)
C(26)	0.231 (2)	-0.088 (1)	0.091 (1)	3.9 (4)
C(27)	0.387 (2)	0.104 (1)	0.2874 (9)	3.1 (3)
C(28)	0.512 (2)	0.056 (1)	0.333 (1)	4.4 (4)
C(29)	0.139 (2)	0.790 (2)	0.299 (1)	5.7 (5)
C(30)	0.030 (2)	0.694 (2)	0.280 (1)	6.4 (5)
B	0.253 (2)	0.100 (2)	-0.124 (1)	3.2 (4)
N(6)	0.118 (3)	0.237 (3)	0.418 (2)	4.9 (6)*
O(6)	0.097 (5)	0.200 (4)	0.510 (3)	11 (1)*
N(8)	0.091 (4)	0.218 (3)	0.097 (2)	5.7 (7)*
O(8)	0.114 (5)	0.251 (3)	0.002 (2)	10 (1)*

\* Starred  $B$  values are for atoms refined isotropically. Anisotropically refined atoms are given in the form of the isotropic equivalent displacement parameter defined as  $(4/3)[a^2B(1,1) + b^2B(2,2) + c^2B(3,3) + ab(\cos \gamma)B(1,2) + ac(\cos \beta)B(1,3) + bc(\cos \alpha)B(2,3)]$ .

(4) Crystal Structure of  $[\text{W}(\text{CO})_3(\text{NO})(\text{C}_{24}\text{H}_{27}\text{N}_5)]\text{BF}_4\cdot\text{CH}_3\text{CN}$  (**4c**). The overall molecular configuration of the complex cation and the atom numbering system are given in Figure 1, while Tables I-IV summarize the crystallographic results.

The crystal structure is composed of discrete units of  $[\text{W}(\text{CO})_3(\text{NO})(\text{C}_{24}\text{H}_{27}\text{N}_5)]^+$  with the  $\text{BF}_4^-$  anions and the  $\text{CH}_3\text{CN}$  solvates distributed in lattice cavities formed by the packing of the cations. As predicted, the major modification that occurs upon formation of **4c** is the transformation of the bidentate unit of **2c** into a tridentate moiety by formation of a supplementary imine

- (28) See for instance: Andrews, M. A.; Kaesz, H. D. *J. Am. Chem. Soc.* **1979**, *101*, 7238; **1979**, *101*, 7255. Andrews, M. A.; van Buskirk, G.; Knobler, C. B.; Kaesz, H. D. *J. Am. Chem. Soc.* **1979**, *101*, 7245. Doney, J. J.; Bergman, R. G.; Heathcock, C. H. *J. Am. Chem. Soc.* **1985**, *107*, 3724. Wright, T. C.; Wilkinson, G.; Motevalli, M.; Hursthouse, M. B. *J. Chem. Soc., Dalton Trans.* **1986**, 2017. Jordan, R. F.; Bajgur, C. S.; Dasher, W. E.; Rheingold, A. L. *Organometallics* **1987**, *6*, 1041. Bochmann, M.; Wilson, L. M.; Hursthouse, M. B.; Motevalli, M. *Organometallics* **1988**, *7*, 1148.

**Table III.** Important Bond Distances (Å) for  $[\text{W}(\text{CO})_3(\text{NO})(\text{C}_{24}\text{H}_{27}\text{N}_5)](\text{BF}_4)\cdot\text{CH}_3\text{CN}$  (**4c**)

Carbonyl Groups			
W-C(1)	1.968 (15)	C(1)-O(1)	1.171 (15)
W-C(2)	2.012 (15)	C(2)-O(2)	1.149 (15)
W-C(3)	1.819 (11)	C(3)-O(3)	1.189 (13)
Nitrosyl Group			
W-N(6)	2.28 (2)	N(6)-O(6)	1.46 (4)
W-N(8)	2.28 (3)	N(8)-O(8)	1.48 (4)
Organic Ligand			
W-N(1)	2.183 (9)	W-N(2)	2.229 (9)
W-N(7)	2.175 (9)	N(7)-C(25)	1.275 (15)
C(25)-C(26)	1.49 (2)	C(25)-C(22)	1.50 (2)
C(22)-C(23)	1.49 (2)	C(22)-C(27)	1.585 (15)
C(23)-C(24)	1.51 (2)	C(27)-C(28)	1.47 (2)
C(23)-N(1)	1.280 (13)	C(27)-N(2)	1.269 (15)
$\text{BF}_4^-$ Anion			
B-F(1)	1.36 (2)	B-F(2)	1.33 (2)
B-F(3)	1.33 (2)	B-F(4)	1.27 (2)
$\text{CH}_3\text{CN}$ Solvate			
N(5)-C(29)	1.15 (2)	C(29)-C(30)	1.47 (3)

**Table IV.** Selected Bond Angles (deg) for  $[\text{W}(\text{CO})_3(\text{NO})(\text{C}_{24}\text{H}_{27}\text{N}_5)](\text{BF}_4)\cdot\text{CH}_3\text{CN}$  (**4c**)

W Coordination			
C(1)-W-C(2)	87.5 (5)	C(1)-W-C(3)	89.5 (5)
C(1)-W-N(1)	173.0 (4)	C(1)-W-N(2)	95.7 (4)
C(1)-W-N(7)	92.3 (4)	C(1)-W-N(6)	52.9 (7)
C(1)-W-N(8)	129.2 (8)	C(2)-W-C(3)	90.4 (4)
C(2)-W-N(1)	96.4 (4)	C(2)-W-N(2)	170.2 (4)
C(2)-W-N(7)	90.0 (4)	C(2)-W-N(6)	127.6 (7)
C(2)-W-N(8)	53.2 (8)	C(3)-W-N(1)	96.3 (4)
C(3)-W-N(2)	98.8 (4)	C(3)-W-N(7)	178.2 (4)
C(3)-W-N(6)	60.6 (7)	C(3)-W-N(8)	117.8 (8)
N(1)-W-N(2)	79.5 (3)	N(1)-W-N(7)	81.9 (3)
N(1)-W-N(6)	127.0 (7)	N(1)-W-N(8)	51.0 (7)
N(2)-W-N(7)	80.7 (4)	N(2)-W-N(6)	60.7 (7)
N(2)-W-N(8)	118.7 (8)	N(7)-W-N(6)	120.4 (7)
N(7)-W-N(8)	61.2 (7)	N(6)-W-N(8)	178 (1)
Carbonyl and Nitrosyl Groups			
W-C(1)-O(1)	177 (1)	W-C(2)-O(2)	173 (1)
W-C(3)-O(3)	177.8 (9)	W-N(6)-O(6)	156 (2)
W-N(8)-O(8)	160 (2)		
$\text{BF}_4^-$ Anion			
F(1)-B-F(2)	113 (1)	F(1)-B-F(3)	112 (1)
F(1)-B-F(4)	106 (1)	F(2)-B-F(3)	106 (1)
F(2)-B-F(4)	113 (2)	F(3)-B-F(4)	106 (2)
$\text{CH}_3\text{CN}$ Solvate			
N(5)-C(29)-C(30)	177 (2)		

appendage, which formally results from the "insertion" of a  $\text{CH}_3\text{C}\equiv\text{N}$  molecule into a  $\text{C}_{\text{sp}}\text{-H}$  bond of the coordinated  $-\text{N}=\text{C}-\text{CH}_2-\text{C}=\text{N}-$  unit (see Scheme I and Figure 1).

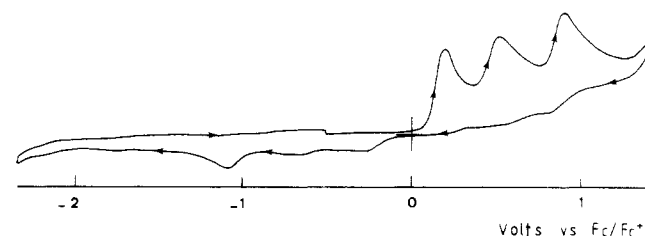
The central tungsten atom is seven-coordinate and has an irregular capped octahedral environment; the three carbonyl groups and three nitrogen atoms [N(1) and N(2) initially bonded to the metal in the tetracarbonyl starting product and the ex- $\text{CH}_3\text{CN}$  N(7) atom] define the distorted octahedron, while the disordered nitrosyl group lies in two opposite capping positions (Figure 1) with statistical occupancy factors of 0.5. The complex cation exhibits approximate  $C_s$  symmetry, the mirror plane being defined by W, N(7), and the carbonyl group C(3)-O(3).

The scorpion tail of the organic ligand arising from the added  $\text{CH}_3\text{CN}$  molecule contains a strong C(25)-N(7) bond [1.275 (15) Å], while the W-N(7) bond length [2.175 (9) Å] has a value very similar to those for W-N(1) [2.183 (9) Å] and W-N(2) [2.229 (9) Å]. Surprisingly, there are strong differences between the W-C bond lengths of the carbonyl groups: the W-C(3) distance of 1.819 (11) Å, in a trans position relative to N(7), is significantly shorter than those observed for W-C(1) [1.968 (15) Å] and W-C(2) [2.012 (15) Å], which are trans to N(1) and N(2), respectively.

**Table V.** Electrochemical Data

(a) Cyclic Voltammetric Data <sup>a</sup>					
complex	redn potential <sup>b</sup>		oxidn potential <sup>b</sup>		
	$E_{r2}$	$E_{r1}$	$E_{a1}$	$E_{a2}$	$E_{a3}$
$[\text{Mo}(\text{CO})_4(\text{L}/\text{H}_2)]$ ( <b>1b</b> )			0.20	0.54	0.91
$[\text{W}(\text{CO})_4(\text{L}/\text{H}_2)]$ ( <b>1a</b> )			0.15 (60)	0.63	0.93
$[\text{Mo}(\text{CO})_3(\text{NO})(\text{C}_{24}\text{H}_{27}\text{N}_5)]\text{BF}_4$ ( <b>4b</b> )		-2.22	0.80	0.99	
$[\text{W}(\text{CO})_3(\text{NO})(\text{C}_{24}\text{H}_{27}\text{N}_5)]\text{BF}_4$ ( <b>4c</b> )		-1.98	0.74	1.04	
$[\text{MoOL}]^+$ ( <b>5b</b> )	-2.22 (60)	-0.73 (60)	0.43 (60)		
$[\text{WOL}]^+$ ( <b>5a</b> )	-2.10 (100)	-0.75	0.25 (80)		
(b) Coulometric Data					
complex	potential of electrolysis, V			$n_{\text{app}}$	
<b>1b</b>	$E_1 = 0.35$			2.47	
<b>1b</b>	$E_1 = 0.40$			2.09	
<b>1b</b>	$E_2 = 0.75$			4.31	
<b>1b</b> + $\text{H}_2\text{O}$	$E_2 = 0.75$			5.00	
<b>1a</b>	$E_2 = 0.77$			2.21	
<b>1a</b> + $\text{H}_2\text{O}$	$E_2 = 0.77$			5.02	

<sup>a</sup>  $\text{C}_6\text{H}_5\text{CN}-0.1$  M  $\text{Bu}_4\text{NPF}_6$ ; Pt electrode; volts vs  $\text{Fc}/\text{Fc}^+$ ; scan rate 200  $\text{mV s}^{-1}$ . <sup>b</sup> Numbers in parentheses refer to  $\Delta E_p$  ( $=E_{\text{pa}} - E_{\text{pc}}$ ) values in mV. Absence of a value indicates the wave was irreversible.

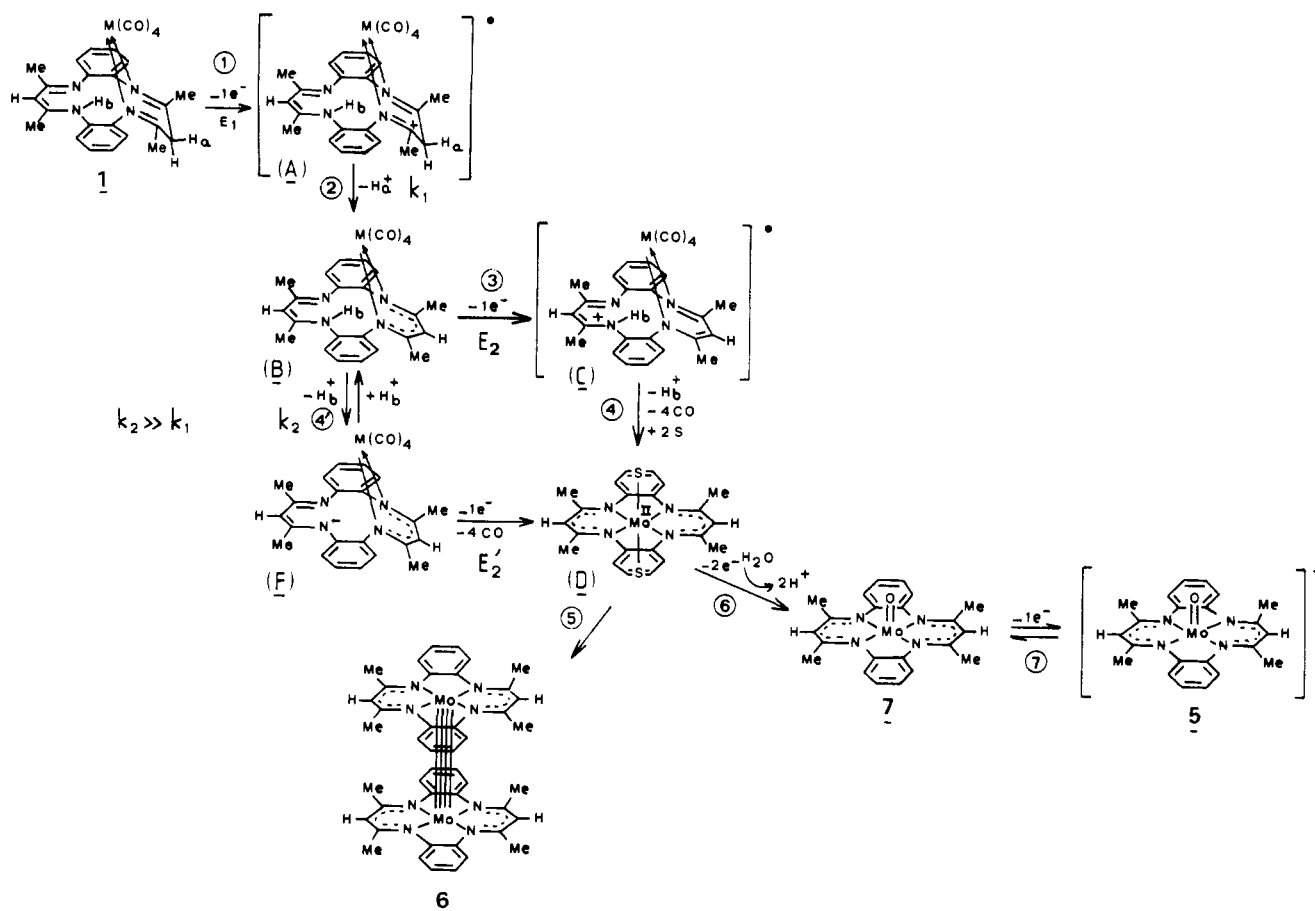
**Figure 3.** Cyclic voltammogram of **1b** ( $\text{C}_6\text{H}_5\text{CN}-0.1$  M  $\text{Bu}_4\text{NPF}_6$ ;  $\nu = 200$   $\text{mV s}^{-1}$ ; potential in V vs  $\text{Fc}^+/\text{Fc}$ ).

As expected, the skeleton of the initial organic ligand has gross distortions from planarity. The four C-N bonds of the *o*-phenylenediamine residues [average length 1.45 (2) Å] have predominant single-bond character and break the electronic delocalization that was primarily limited to the benzene rings and the N-C-C-C-N units. The uncoordinated N(3)-C(11)-C(13)-C(14)-N(4) fragment has a planar imine-enamine double-bond arrangement with a delocalization similar to that observed in the free ligand  $\text{LH}_2$  [bond lengths (Å) in **4c** with the corresponding mean value observed in  $\text{LH}_2$ <sup>14</sup> given in brackets: N(3)-C(11) = 1.31 (2) [1.316 (3)]; C(11)-C(13) = 1.44 (2) [1.414 (3)]; C(13)-C(14) = 1.38 (2) [1.376 (3)]; C(14)-N(4) = 1.35 (2) [1.343 (3)]]. Due to the presence of the  $\text{sp}^3$  C(22) carbon atom, the coordinated N(1)-C(23)-C(22)-C(27)-N(2) unit appears as a nonplanar fragment with two carbon-nitrogen double bonds [N(1)-C(23) = 1.280 (13) Å; N(2)-C(27) = 1.269 (15) Å] and two carbon-carbon single bonds [C(23)-C(22) = 1.49 (2) Å; C(22)-C(27) = 1.585 (15) Å].

The two different positions statistically occupied by the nitrosyl ligand present similar features [W-N(6) = 2.28 (2); N(6)-O(6) = 1.46 (4) Å; W-N(6)-O(6) = 156 (2)° vs W-N(8) = 2.28 (3) Å; N(8)-O(8) = 1.48 (4) Å; W-N(8)-O(8) = 160 (2)°]. The M-N and N-O bond lengths values are unusually large although they may be compared with the corresponding values in the nitrosylcobalt complex  $\text{Na}_4\text{Si}_{12}\text{Al}_{12}\text{O}_{48}\text{Co}_4(\text{NO})_3$  [Co-N = 2.23 (6) Å; N-O = 1.47 (11) Å].<sup>29</sup> These values may be at least partially explained by the capping position occupied by the NO group in this crowded seven-coordinate complex.

The geometries of the  $\text{BF}_4^-$  anion and the  $\text{CH}_3\text{CN}$  solvate molecule reveal no unexpected features.

**(5) Electrochemistry.** The unusual  $\text{L}/\text{H}_2$  form of the macrocycle in the complexes **1** and **2** prompted us to investigate their electrochemical behavior. Electrochemical studies of  $[\text{M}^{\text{II}}\text{L}]$  deriv-

Scheme II. Postulated Mechanism for the Transformation 1 → 5<sup>a</sup>

<sup>a</sup> Letters A-F refer to nonisolated intermediates, while numbers refer to solid-state-characterized complexes. Complexes 1,<sup>23</sup> 5,<sup>32</sup> and 6<sup>24</sup> have been characterized by X-ray structure determinations. Complex 7 has been characterized by <sup>1</sup>H NMR and CV studies.<sup>31</sup> S = C<sub>6</sub>H<sub>5</sub>CN.

atives are widespread in the literature.<sup>30</sup>

Table V summarizes the electrochemical results obtained for these complexes by cyclic voltammetry (CV). The carbonyl compounds **1** show three monoelectronic oxidation peaks (Figure 3), all electrochemically irreversible except the first redox process of **1a**, which is reversible. On the cathodic scale, no reduction reaction is observed.

Controlled-potential electrolyses have been carried out at potentials corresponding to the first (*E*<sub>1</sub>) and second (*E*<sub>2</sub>) oxidation processes. Whatever the potential may be, the yellow starting solutions of **1** always turn either to an orange (**1a**) or a greenish color (**1b**) after electron removal. For the different electrolyses carried out in carefully dried benzonitrile (C<sub>6</sub>H<sub>5</sub>CN), the experimental values of *n*<sub>app</sub> are not reproducible, fluctuating between 2 and 5 electrons; moreover, log *i* vs *t* curves display complicated behavior. By comparison of its cyclic voltammogram and its ESR spectrum<sup>31</sup> with those of an authentic chemically synthesized sample, the major product arising from electrochemical oxidations of **1b** was shown to be the oxomolybdenum(V) cation [MoOL]<sup>+</sup> (**5b**), for which an X-ray structural determination indicated the presence of the usual tetradentate L<sup>2-</sup> ligand.<sup>32</sup> The cyclic voltammograms of the solutions obtained by electrolysis of **1a** and

**1b** exhibit similar features (Table V), and the formula [WOL]<sup>+</sup> was therefore assigned to the main electrochemically oxidized compound **5a** arising from **1a**.

Residual water in the solvent was suspected as the oxygen source, and the effect resulting from addition of water was thus examined. The presence of water in benzonitrile (ca. 2 μL of H<sub>2</sub>O/500 μL of C<sub>6</sub>H<sub>5</sub>CN) has practically no effect on the CV of compounds **1**, the most anodic peak only being slightly affected, but this could be due to the water oxidation process; however, it is noteworthy that exhaustive coulometries performed with a slight excess of water end in the abstraction of 5 electrons in a reproducible way (Table V). In the corresponding voltammograms, the peaks of the resulting oxo complex lose their diffuse shape and increase in intensity. These observations clearly indicate that the *n* value of 5 electrons corresponds to the overall electronic conversion process **1** → **5** and establish that H<sub>2</sub>O acts as an oxo donor. Furthermore, CV results show that, to begin with, 2 electrons can be successively withdrawn from **1** to yield a very reactive species, shown by the irreversibility of these two processes, which appear as closely interdependent, since the final product of the electrolysis does not depend on the selected potential (*E*<sub>1</sub> or *E*<sub>2</sub>).

## Discussion

From these data and the chemical reactivity of complexes **1** reported in sections 1 and 2, the mechanism shown in Scheme II may be postulated for the transformation of **1** into **5**. First, the monoelectronic oxidation (*E*<sub>1</sub>) of **1** gives the radical complex A, which, via deprotonation at the sp<sup>3</sup> carbon atom (by comparison with reaction ii—see section 2), would afford the species B. Abstraction of a second electron leads to C, which would be sufficiently acidic to give, following step 4, the pseudooctahedral mononuclear species [ML(C<sub>6</sub>H<sub>5</sub>CN)<sub>2</sub>] (D) containing a Mo(II)

- (30) McElroy, F. C.; Dabrowiak, J. C. *J. Am. Chem. Soc.* **1976**, *98*, 7112. Dabrowiak, J. C.; Fisher, D. P.; McElroy, F. C.; Macero, D. *Inorg. Chem.* **1979**, *18*, 2304. Bailey, C. L.; Bereman, R. D.; Rillema, D. P.; Nowak, R. *Inorg. Chem.* **1984**, *23*, 3956. Bailey, C. L.; Bereman, R. D.; Rillema, D. P.; Novak, R. *Inorg. Chim. Acta* **1986**, *116*, L45. Bailey, C. L.; Bereman, R. D.; Rillema, D. P. *Inorg. Chem.* **1986**, *25*, 3149.
- (31) Giraudon, J. M.; Guerschais, J. E.; Sala-Pala, J.; Toupet, L. To be published.
- (32) Giraudon, J. M.; Guerschais, J. E.; Sala-Pala, J.; Toupet, L. *J. Chem. Soc., Chem. Commun.* **1988**, 921.

cation and a tetradentate  $L^2$ -ligand. It has been recently reported that reduction of the mononuclear Mo(IV) complex  $[Mo(acacen)Cl_2]$  with sodium sand in the presence of diphenylacetylene affords the diamagnetic Mo(II) dimer  $[Mo(acacen)]_2$  containing an Mo–Mo quadruple bond, while reduction in the absence of  $Ph_2C_2$  gives different results that are currently under investigation.<sup>33</sup> By comparison, we presume D has a high reactivity and could dimerize or react with adventitious incoming reactive species. It is noteworthy that dimerization of D would give the dinuclear complex **6** that we have previously reported.<sup>24</sup> However, in the current medium D would react with water to produce first the previously known oxo compound **7**<sup>32</sup> and then, via a new oxidation process, the X-ray characterized oxometal(V) cationic complex **5**.<sup>32</sup> Observation that oxidations at peak 1 or peak 2 both yield complex **5** can be explained by the acid–base equilibrium **4'**, the resulting basic entity F being very likely oxidizable at a potential  $E'_2 < E_1$ . This is in agreement with the disappearance of the second process when the microelectrolyses are carried out at an anodic potential vs peak 1 and cathodic potential vs peak 2.

It is of interest to note that the conversion of **6** into **5** by reaction with TCNE in the presence of traces of water, which we observed recently,<sup>32</sup> was thought to involve the dinuclear radical cation  $[Mo_2L_2]^{*+}$  (and not the species D) as an intermediate.

### Concluding Remarks

In summary, it can be concluded that tetramethyldibenzo-tetraaza[14]annulene may act as a versatile ligand much more readily than previously thought. In the cationic nitrosyl complexes  $[M(CO)_3(NO)(C_{22}H_{24}N_4)]^+$  (cations of **2**), as in the starting tetracarbonyl complexes  $[M(CO)_4(C_{22}H_{24}N_4)]$  (**1**), the organic unit intervenes as a neutral bidentate  $L'H_2$  ligand arising from the free organic molecule  $LH_2$  via a hydrogen transfer from a nitrogen atom to a carbon atom. The reaction at room temperature of the nitrosyl complexes with acetonitrile induces the transformation of the bidentate ligand  $L'H_2$  into a novel tridentate ligand, which contains a scorpion tail resulting from a pseudoinsertion of  $CH_3CN$  into a CH bond.

Electrochemical oxidation of the tetracarbonyl derivatives  $[M(CO)_4(L'H_2)]$  (**1**) affords the oxocationic complexes  $[MOL]^+$  (**5**), in which the deprotonated ligand has its usual tetradentate coordination mode. Careful analysis of the electrochemical data indicates that residual water in the solvent is the source of oxygen.

### Experimental Section

**(1) Preparative Studies and Physical Measurements.** Reactions were performed in Schlenk tubes in a dry oxygen-free dinitrogen atmosphere. Solvents were distilled by standard methods and thoroughly deoxygenated before use. Elemental analyses were performed by the "Service Central d'Analyse du CNRS". IR spectra were recorded on a Perkin-Elmer 1430 spectrophotometer. <sup>1</sup>H NMR spectra were run on a Jeol FX 100 spectrophotometer and are referred to TMS. Mass spectra were obtained with a Varian Mat 311 mass spectrophotometer ("Centre de Mesures Physiques", Rennes, France).

$TMTAAH_2^5$  and  $[M(CO)_4(TMTAAH_2)]^{22}$  ( $M = Mo, W$ ) were prepared by published procedures.

**Synthesis of the Nitrosyl Complexes  $[M(CO)_3(NO)(C_{22}H_{24}N_4)]Y$  (**2a**,  $M = W$ ,  $Y = PF_6$ ; **2b**,  $M = Mo$ ,  $Y = BF_4$ ; **2c**,  $M = W$ ,  $Y = BF_4$ ).** All these complexes were prepared similarly. To a stirred solution of  $[W(CO)_4(C_{22}H_{24}N_4)]$  (**1a**) (618 mg, 1.06 mmol) in dichloromethane was added at  $-50^\circ C$   $NOPF_6$  (185 mg, 1.06 mmol). The yellow solution was slowly allowed to warm up; it became purple at ca.  $-40^\circ C$  and was stirred for 8 h at room temperature. The solvent was removed under reduced pressure and the residue washed with pentane. Extraction with dichloromethane followed by filtration through Celite and addition of pentane to the filtrate gave **2a** as purple microcrystals. The yield of complexes **2** was 80–90%. Complexes **2** are thermally stable and slightly air-sensitive in the solid state.

**2a.** <sup>1</sup>H NMR  $[(CD_3)_2CO]$ :  $\delta$  2.09 (6 H, s,  $CH_3$ ), 2.34 (6 H, s,  $CH_3$ ), 2.26 (1 H, d,  $J = 14.1$  Hz) and 2.53 (1 H, d,  $J = 14.1$  Hz) [ $CH_2$  (AB system)], 4.93 (1 H, s, CH), 7.32 (8 H, m, Ar H), 12.93 (1 H, s, NH). IR (KBr): 2020 s and 1940 vs  $\nu(CO)$ , 1650 vs  $\nu(NO)$ , 1615 s  $\nu(N=C-N)$ , 850 vs  $\nu(PF)$ , 560 m  $\delta(PFP)$   $cm^{-1}$ .

$\nu(N=C-N)$ , 850 vs  $\nu(PF)$ , 560 m  $\delta(PFP)$   $cm^{-1}$ .

**2b.** Anal. Calcd for  $C_{25}H_{24}N_5O_4MoBF_4$ : C, 46.8; H, 3.8; N, 10.9. Found: C, 47.4; H, 4.1; N, 11.1. <sup>1</sup>H NMR  $[(CD_3)_2CO]$ :  $\delta$  2.05 (6 H, s,  $CH_3$ ), 2.29 (6 H, s,  $CH_3$ ), 4.95 (1 H, s, CH), 7.31 (8 H, s, Ar H), 12.3 (1 H, s, NH) [due to low solubility, the  $CH_2$  resonances (AB system) appear as poorly resolved signals]. IR (KBr): 2020 s and 1950 vs  $\nu(CO)$ , 1660 vs  $\nu(NO)$ , 1615 s  $\nu(N=C-N)$ , 1080 vs br  $\nu(BF)$   $cm^{-1}$ .

**2c.** Anal. Calcd for  $C_{25}H_{24}N_5O_4WBF_4$ : C, 41.2; H, 3.3; N, 9.6. Found: C, 41.3; H, 3.7; N, 10.2. <sup>1</sup>H NMR  $[(CD_3)_2SO]$ :  $\delta$  2.03 (12 H, s,  $CH_3$ ), 4.90 (1 H, s, CH), 7.45 (8 H, s, Ar H), 12.7 (1 H, s, NH) [due to low solubility, the  $CH_2$  resonances (AB system) appear as poorly resolved signals]. IR (KBr): 2015 s and 1920 vs  $\nu(CO)$ , 1640 vs  $\nu(NO)$ , 1620 s  $\nu(N=C-N)$ , 1070 vs br  $\nu(BF)$   $cm^{-1}$ .

**Deprotonation of the Nitrosyl Complexes **2**. Formation of  $[M(CO)_3(NO)(C_{22}H_{23}N_4)]$  (**3a**,  $M = W$ ; **3b**,  $M = Mo$ ).** To a stirred solution of  $[W(CO)_3(NO)(C_{22}H_{24}N_4)]BF_4$  (**2c**) (473 mg, 0.6 mmol; THF;  $-65^\circ C$ ) was added an excess of *t*-BuOK (151 mg, 1.34 mmol) [*t*-BuLi may be used instead of *t*-BuOK]. The deep red solution was allowed to warm up, and it darkened at ca.  $-50^\circ C$ . The solvent was then removed under reduced pressure at room temperature and the residue extracted with  $CH_2Cl_2$ . After filtration through Celite, pentane was added to the filtrate. The resulting precipitate was filtered out, copiously washed with an ether–pentane (70–30) mixture, and dried in vacuo. Yield: ca. 20%.

**3a.** Anal. Calcd for  $C_{25}H_{23}N_5O_4W$ : C, 46.9; H, 3.6; N, 10.9; W, 28.7. Found: C, 44.0; H, 4.0; N, 11.1; W, 28.8. <sup>1</sup>H NMR  $(CD_2Cl_2)$ :  $\delta$  1.88 (6 H, s,  $CH_3$ ), 2.00 (6 H, s,  $CH_3$ ), 4.73 (2 H, m, CH), 7.20 (8 H, m, Ar H), 13.0 (1 H, s, NH). IR (KBr): 2000 s and 1900 vs  $\nu(CO)$ , 1620 s  $\nu(NO)$   $cm^{-1}$ .

**3b** exhibits similar spectroscopic data.

**Protonation of Complexes **3**.** To a THF solution of **3a** (1025 mg, 1.6 mmol) at  $-80^\circ C$  was added  $HBF_4 \cdot O(C_2H_5)_2$  (213  $\mu L$ , 1.6 mmol). After warming to room temperature, the solvent was removed under reduced pressure and the residue washed with pentane. Extraction with  $CH_2Cl_2$  followed by addition of pentane gave a precipitate that on the basis of its spectroscopic data was identified as **2c**.

Protonation of **3a** was also obtained by HCl bubbling at  $-20^\circ C$ . The corresponding chloride complex precipitated; it was washed with pentane and dried in vacuo.

**Reaction of Complexes **2** with Acetonitrile. Formation of  $[M(CO)_3(NO)(C_{24}H_{27}N_5)]BF_4$  (**4b**,  $M = Mo$ ; **4c**,  $M = W$ ).** A clear  $CH_3CN$  solution of  $[M(CO)_3(NO)(C_{22}H_{24}N_4)]BF_4$  (ca. 1.5 g in 50 mL) gave, after standing for ca. 24 h at room temperature, crystals, which were filtered out and washed with acetonitrile and pentane. Yield: ca. 80%.

**4b.** Anal. Calcd for  $C_{27}H_{27}N_6O_4MoBF_4 \cdot H_2O$ : C, 46.3; H, 4.2; N, 12.0. Found: C, 46.0; H, 4.3; N, 11.0. <sup>1</sup>H NMR  $[(CD_3)_2CO]$ :  $\delta$  2.09 (6 H, s,  $CH_3$ ), 2.11 (6 H, s,  $CH_3$ ), 2.39 (3 H, s,  $CH_3-C=NH$ ), 5.05 (1 H, s,  $HC_{13}^*$ ), 6.30 (1 H, s,  $HC_{22}^*$ ), 7.28 (8 H, m, Ar H), 11.45 (1 H, s,  $HN_7^*$ ), 12.98 (1 H, s,  $HN_4^*$ ) (asterisk indicates labeling of atoms like that for **4c**; see Figure 1). IR (KBr): 2025 s and 1940 vs  $\nu(CO)$ , 1670 vs  $\nu(NO)$   $cm^{-1}$ .

**4c.** Anal. Calcd for  $C_{27}H_{27}N_6O_4WBF_4 \cdot CH_3CN$ : C, 43.0; H, 3.7; N, 12.1; B, 1.3. Found: C, 42.9; H, 3.7; N, 12.1; B, 1.3. <sup>1</sup>H NMR  $[(CD_3)_2SO]$ :  $\delta$  2.03 (6 H, s,  $CH_3$ ), 2.06 (3 H, s,  $CH_3CN$  solvate), 2.22 (6 H, s,  $CH_3$ ), 2.56 (3 H, s,  $CH_3-C=NH$ ), 4.97 (1 H, s,  $HC_{13}^*$ ), 6.25 (1 H, s,  $HC_{22}^*$ ), 7.24 (8 H, m, Ar H), 11.96 (1 H, s,  $HN_7^*$ ), 12.80 (1 H, s,  $HN_4^*$ ) (asterisk indicates labeling of atoms as in Figure 1). IR (KBr): 2010 s, 1935 vs  $\nu(CO)$ , 1670 vs  $\nu(NO)$ , 1070 vs  $\nu(BF)$   $cm^{-1}$ .

**(2) X-ray Crystallographic Study of **4c**.** Yellow crystals of **4c** were grown from a dry acetonitrile solution stored under nitrogen. Preliminary studies indicated that the crystals were unstable and decomposed within a few hours in the X-ray beam at room temperature. Accordingly, a first crystal (approximate dimensions  $0.2 \times 0.1 \times 0.1$  mm) was mounted on a glass fiber. Data were collected with the  $\theta$ – $2\theta$  scan technique at 138 K ( $\tau_{max} = 60$  s). The intensities of two strong reflections were measured periodically; although no detectable deterioration of the crystal was observed in the first hours, the crystal decomposed suddenly after 1757 independent reflections ( $h = -8 \rightarrow 8$ ;  $k = -12 \rightarrow 12$ ;  $l = 0 \rightarrow 3$ ) were collected. After data reduction including Lorentz and polarization corrections, 1345 reflections having  $I > 3\sigma(I)$  were classed as observed.

The position of the tungsten atom was determined from a Patterson synthesis, and those of the remaining non-hydrogen atoms (except those of the  $CH_3CN$  solvate) were determined from subsequent difference Fourier syntheses. At this stage ( $R = 0.095$ ), the anisotropic thermal parameters were not clearly defined; therefore, a second crystal was mounted and the intensity data collected with a greater scan speed ( $\tau_{max} = 40$  s;  $h = -8 \rightarrow 8$ ;  $k = -11 \rightarrow 11$ ; first with  $l = 4 \rightarrow 13$  and then  $l = 1$  and  $l = 2$ ; at this time the crystal decomposed suddenly). If both crystals are taken into account, on 4394 observed data, 2053 reflections having net intensities  $I > 3\sigma(I)$  were observed and the refinement was based on these reflections. At this stage, empirical absorption correction

(33) Pennesi, G.; Floriani, C.; Chiesi-Villa, A.; Guastini, C. *J. Chem. Soc., Chem. Commun.* 1988, 350.

was performed by using the program DIFABS.<sup>34</sup> The nitrosyl group appeared to occupy two general positions with a statistical occupancy of 0.5, and the corresponding N and O atoms [and also the C(3) atom] were refined with isotropic temperature factors, while the remaining non-hydrogen atoms were refined with anisotropic thermal parameters. Hydrogen atoms were added at calculated positions and included in the structure factor calculations. Attempts to correct the data for secondary extinction gave no significant result. Refinement was on  $F$  with  $\sigma$  weights,  $1/\sigma^2(F_o)$ . The  $R$  and  $R_w$  values corresponding to the final cycle of full-matrix least-squares refinement are given in Table I.

Neutral-atom scattering factors were taken from Cromer and Waber;<sup>35</sup> those for tungsten were corrected for anomalous dispersion.<sup>36</sup> All calculations were performed with the Enraf-Nonius CAD4 SDP programs.<sup>37</sup>

(3) **Electrochemistry.** The solvent (benzonitrile) and the supporting electrolyte ( $\text{Bu}_4\text{NPF}_6$ ) were purified as described earlier.<sup>38</sup> As some redox states of the compounds under study are very reactive toward oxygen, all of the experiments were conducted inside a nitrogen-atmosphere box,  $\text{N}_2$  being purified continuously by passage through molecular sieves and BTS catalyst. As the presence of residual water affects the

voltammograms of these compounds greatly, solutions of the supporting electrolyte (0.1 M  $\text{Bu}_4\text{NPF}_6$ ) were prepared in the box, stored over molecular sieves (Linde 4A), and dried just before use by two successive percolations through activated (400 °C under vacuum for 48 h) neutral alumina (Merck) columns. From the observation of the effect of added water on the background current, the concentration of residual water in the electrolyte solution is estimated to be less than 0.05 mM.

**Apparatus.** A three-compartment microelectrochemical cell has been specially designed. The platinum (2 mm) or glassy-carbon (3 mm) rotating-disk electrode (EDI-Tacussel) is adapted to the main compartment through a ground joint (14.5/23). The auxiliary and reference electrodes are connected at the bottom of the cell via ground joints (7/16); they are terminated by Vycor tips (PAR). Such a cell allows cyclic and rotating-disk voltammetry to be performed on 0.3–0.5 mL of solution. The small volume of solution can be electrolyzed completely, directly in the same cell, by using the rotating-disk electrode.

The reference electrode used is the half-cell: Pt/ferrocenium picrate ( $10^{-2}$  M), ferrocene ( $10^{-2}$  M),  $\text{Bu}_4\text{NPF}_6$  (0.2 M), benzonitrile. For comparison of the present results with other work, the  $\text{Fc}/\text{Fc}^+$  formal potential has been measured versus SCE in benzonitrile (0.2 M  $\text{Bu}_4\text{NPF}_6$ ):  $E^\circ(\text{Fc}/\text{Fc}^+) = +0.43$  V vs SCE.

A Model 173 potentiostat (PAR) monitored by a Model 175 programmer (PAR) and a T2-Y x-y chart recorder (Sefram-Enertec) were used for the electrochemical investigations.

**Acknowledgment.** We thank the DRET for financial support of this research.

**Supplementary Material Available:** Tables of general temperature factor expressions  $U^2$ s, bond distances and bond angles for the  $\text{C}_{24}\text{H}_{27}\text{N}_5$  ligand, and least-squares planes (7 pages); a table of observed and calculated structure factors (13 pages). Ordering information is given on any current masthead page.

(34) Walker, N.; Stuart, D. *Acta Crystallogr.* **1983**, *A39*, 159.

(35) Cromer, D. T.; Waber, J. T. *International Tables for X-Ray Crystallography*; Kynoch Press: Birmingham, England, 1974; Vol. IV, Table 2.2B.

(36) Cromer, D. T. *International Tables for X-Ray Crystallography*; Kynoch Press: Birmingham, England, 1974; Vol. IV, Table 2.3.1.

(37) Frenz, B. A. "Enraf-Nonius Structure Determination Package", Delft University Press, Delft, Holland, 1985.

(38) Le Mest, Y.; L'Her, M.; Courtot-Coupez, J.; Collman, J. P.; Evitt, E. R.; Bencosme, C. S. *J. Electroanal. Chem. Interfacial Electrochem.* **1985**, *184*, 331.

Contribution from the Department of Chemistry and Biochemistry, University of California, Los Angeles, California 90024-1569

## Synthesis and Characterization by $^1\text{H}$ , $^{13}\text{C}$ , and $^{19}\text{F}$ NMR Spectroscopy of $(\text{CH}_3\text{CN})_n(\text{CO})_{4-n}(\text{NO})\text{W}(\mu\text{-F})\text{BF}_3$ and $[(\text{CH}_3\text{CN})_{n+1}(\text{CO})_{4-n}(\text{NO})\text{W}][\text{BF}_4]$ ( $n = 0-2$ ), Tungsten Mononitrosyl Carbonyl Cations with Labile Acetonitrile and $[(\mu\text{-F})\text{BF}_3]^-$ Ligands

William H. Hersh<sup>†</sup>

Received June 8, 1989

Addition of  $[\text{NO}][\text{BF}_4]$  to  $\text{CH}_3\text{CNW}(\text{CO})_5$  in  $\text{CH}_2\text{Cl}_2$  gives a mixture of five mononitrosyl compounds, *mer*-(*cis*- $\text{CH}_3\text{CN}$ )-(trans-NO)(CO)<sub>3</sub>W( $\mu\text{-F}$ )BF<sub>3</sub> (1), [*mer*,*cis*-( $\text{CH}_3\text{CN}$ )<sub>2</sub>W(CO)<sub>3</sub>(NO)][BF<sub>4</sub>] (2a), *cis*,*cis*,*trans*-( $\text{CH}_3\text{CN}$ )<sub>2</sub>(CO)<sub>2</sub>(NO)W( $\mu\text{-F}$ )BF<sub>3</sub> (3), [*fac*-( $\text{CH}_3\text{CN}$ )<sub>3</sub>W(CO)<sub>2</sub>(NO)][BF<sub>4</sub>] (4a), and *trans*-(NO)(CO)<sub>4</sub>W( $\mu\text{-F}$ )BF<sub>3</sub> (5); in a typical experiment the yield is 90%, and the ratio 1:2a:3:4a:5 is 47:14:11:1:27. Addition of acetonitrile to the mixture results in substitution of the  $[(\mu\text{-F})\text{BF}_3]^-$  ligand of 1, 3, and 5 with conversion to 2a, 4a, and [*trans*-( $\text{CH}_3\text{CN}$ )W(CO)<sub>4</sub>NO][BF<sub>4</sub>] (6), respectively; allowing the mixture to stand in the presence of excess acetonitrile results in complete conversion of 2a and 6 to 4a. Further support for the identities of 1–5 is obtained by reaction of the mixture with  $\text{Me}_3\text{P}$ , giving [*mer*-(*cis*- $\text{CH}_3\text{CN}$ )-(trans- $\text{Me}_3\text{P}$ )W(CO)<sub>3</sub>(NO)][BF<sub>4</sub>] (7a), [*cis*,*cis*-( $\text{CH}_3\text{CN}$ )<sub>2</sub>(CO)<sub>2</sub>(NO)W( $\text{PMe}_3$ )][BF<sub>4</sub>] (8a), [*trans*- $\text{Me}_3\text{P}$ (CO)<sub>4</sub>WNO][BF<sub>4</sub>] (9), and the previously reported compound [*mer*,*cis*-( $\text{Me}_3\text{P}$ )<sub>2</sub>W(CO)<sub>3</sub>(NO)][BF<sub>4</sub>] (10a). The reaction mixtures are analyzed by IR and  $^1\text{H}$ ,  $^{13}\text{C}$ , and  $^{19}\text{F}$  NMR spectroscopy. In particular, the  $^{13}\text{C}$  NMR spectrum exhibits quintets for the carbonyl ligands of 1, 3, and 5 due to a dynamic "spinning" process of the  $[(\mu\text{-F})\text{BF}_3]^-$  ligand, and the  $^{19}\text{F}$  NMR spectrum exhibits doublets for the terminal fluorine atoms (which are further separated into  $^{10}\text{B}$  and  $^{11}\text{B}$  isotopomers) near -153 ppm and quartets for the bridging fluorine atoms from -203 to -238 ppm. Independent synthesis and isolation in good yield of 2b–c, 4a–d, 7b–c, and 8b (where the anions for a–d are  $[\text{BF}_4]^-$ ,  $[\text{SbF}_6]^-$ ,  $[(\text{C}_6\text{H}_5)_4\text{B}]^-$ , and  $[\text{PF}_6]^-$ , respectively) are described, as are the independent synthesis and spectroscopic characterization of 3, 5, and 6.

### Introduction

Mononuclear tungsten carbonyl complexes have been studied intensively over the years, in part due to their relatively high thermal stability.<sup>1</sup> The octahedral  $d^6$  complexes are both coordinatively and electronically saturated and so for instance serve as ideal templates for stabilizing reactive organic fragments such as carbenes and carbynes.<sup>2</sup> This high stability makes such complexes unlikely candidates for catalysis, however, and with

the exception of the olefin metathesis reaction—where the ligand sphere of the tungsten carbonyl catalyst precursor may be quite different from the ligand sphere of the catalyst<sup>3</sup> that forms in the

(1) (a) Angelici, R. J. *Organomet. Chem. Rev.* **1968**, *3*, 173–226. (b) Dobson, G. R. *Acc. Chem. Res.* **1976**, *9*, 300–306.

(2) See for instance: (a) Fischer, E. O. In *Advances in Organometallic Chemistry*; Stone, F. G. A., West, R., Eds.; Academic Press: New York, 1976; Vol. 14, pp 1–32. (b) Casey, C. P.; Burkhardt, T. J.; Bunnell, C. A.; Calabrese, J. C. *J. Am. Chem. Soc.* **1977**, *99*, 2127–2134. (c) Birdwhistell, K. R.; Tonker, T. L.; Templeton, J. L. *Ibid.* **1985**, *107*, 4474–4483. (d) McDermott, G. A.; Dorries, A. M.; Mayr, A. *Organometallics* **1987**, *6*, 925–931.

<sup>†</sup> Present address: Department of Chemistry and Biochemistry, Queens College of the City University of New York, Flushing, NY 11367-0904.